Journal of Experimental Marine Biology and Ecology 457 (2014) 151–159

Contents lists available at ScienceDirect

Journal of Experimental Marine Biology and Ecology

journal homepage: www.elsevier.com/locate/jembe

Photosynthesis and respiration in marine phytoplankton: Relationship with cell size, taxonomic affiliation, and growth phase

Daffne C. López-Sandoval [a,b,*], Tamara Rodríguez-Ramos [a], Pedro Cermeño [b], Cristina Sobrino [a], Emilio Marañón [a]

[a] Departamento de Ecología y Biología Animal, Universidad de Vigo, 36310 Vigo, Spain
[b] Instituto de Ciencias del Mar, Consejo Superior de Investigaciones Cientificas, Passeig Maritim de la Barceloneta 37–49, 08003 Barcelona, Spain

ARTICLE INFO

Article history:
Received 16 October 2013
Received in revised form 10 April 2014
Accepted 11 April 2014
Available online xxxx

Keywords:
Growth phase
Metabolism
Phytoplankton taxonomic groups
Size-scaling

ABSTRACT

We determined the rates of photosynthesis and respiration in batch cultures of 22 marine phytoplankton species from five phyla covering a range of 7 orders of magnitude in cell size. Rates were determined during the exponential growth phase and also during the stationary phase, when cell growth was limited by nitrogen availability. We observed, in all growth phases, a curvature in the size scaling of carbon fixation, such that the relationship between carbon-specific photosynthesis and cell size was unimodal, with the highest rates being measured in intermediate-size species. The log–log relationship between individual metabolic rates and cell size showed an overall lineal pattern with a slope equal or near 1, irrespective of whether volume or carbon is used as a metric for cell size. Thus, our results demonstrate that when small species (<50 μm^3 cell diameter) are considered together with intermediate- and large-sized species phytoplankton metabolism does not follow Kleiber's 3/4-power rule. Considering all species together, respiration losses represented on average 9% and 22% of total carbon fixation during the exponential growth and stationary phases, respectively. Carbon-specific respiration was largely independent of cell size and growth phase, but tended to take higher values in the dinoflagellates. During the stationary growth phase, and contrary to other groups, most diatoms were able to maintain carbon fixation rates similar to those measured during exponential growth. Our results highlight the ability of intermediate-to-large size species to sustain high metabolic rates in spite of their cell size, which helps to explain why they dominate phytoplankton blooms in the ocean.

1. Introduction

The basic observation that small organisms tend to have higher growth rates and biomass-specific metabolic rates than larger organisms has driven the search for universal scaling laws that could explain the flux of energy through individuals and, by extension, communities and ecosystems (Brown et al., 2004). Size-scaling relationships can be represented using power functions such as:

$$R = aM^b \quad (1)$$

where R is an individual metabolic rate, M is body size (mass or volume), b is the size-scaling exponent and a is a coefficient. After taking logarithms, Eq. (1) can also be written as:

$$\log R = \log a + b \log M \quad (2)$$

where b is the slope of the linear function. Since Kleiber first reported that metabolic rates in birds and mammals scale with body mass with a b value of 3/4 (Kleiber, 1932), this allometric relationship has proven to be applicable to a wide range of organisms, from unicells to multicellular organisms including large plants and animals (Savage et al., 2004).

Phytoplankton cell size, which ranges over more than 9 orders of magnitude, from <1 μm^3 in the smallest cyanobacteria to >10^9 μm^3 in the largest diatoms, can have a large effect on different metabolic rates (Chisholm, 1992; Finkel et al., 2010). It is unclear, however, to which extent Kleiber's rule can be applied to phytoplankton. While several studies have confirmed the applicability of the 3/4-power rule for phytoplankton carbon fixation (Blasco et al., 1982; López-Urrutia et al., 2006; Taguchi, 1976) and respiration (Blasco et al., 1982; Laws, 1975), some others have found size-scaling relationships with b values that deviate significantly from 3/4. In some cases, the values of b obtained were lower than 3/4, which implied a stronger decrease of metabolic rates with increasing cell size (Finkel et al., 2004), whereas in other studies b was higher than 3/4, indicating a smaller degree of size-dependence (Banse, 1976; Lewis, 1989). Recently, field-based studies have reported b values not significantly different from 1 (Huete-Ortega et al., 2012; Marañón, 2008; Marañón et al., 2007).

* Corresponding author at: Departamento de Ecoloxía e Bioloxía Animal, Universidade de Vigo, 36210 Vigo, Spain. Tel.: +34 986 812629.
E-mail address: daffne@uvigo.es (D.C. López-Sandoval).

http://dx.doi.org/10.1016/j.jembe.2014.04.013
0022-0981/

These isometric size-scaling relationships mean that individual metabolic rates are directly proportional to cell size, and therefore that biomass-specific metabolic rates in phytoplankton are independent of cell size. However, there are methodological uncertainties involved in the determination of size-dependent metabolic rates in natural assemblages. For instance, one possibility is that a stronger grazing pressure upon smaller cells during experimental incubations may bias the slope values of the resulting size-scaling relationships.

The different results obtained in previous studies may have been due to variability in experimental methods, the use of different ranges in cell size, the presence of sub-optimal growth conditions, or the fact that the species studied belonged to a single taxonomic group and/or covered a relatively narrow range in cell size. This uncertainty over the size-scaling of phytoplankton metabolism and growth is particularly relevant, since ocean ecological models often require the representation of size-dependent physiological traits of phytoplankton (Armstrong, 1994; Irwin et al., 2006; Ward et al., 2012) but rely on the use of size-scaling parameters obtained from literature reviews (Litchman et al., 2007; López-Urrutia et al., 2006). While undoubtedly useful to provide general patterns, these literature-based studies, however, suffer from the lack of methodological consistency among studies and the disparate growth conditions of the cultures used, which often results in noisy size-scaling relationships with a large amount of unexplained variance.

Elucidating whether or not the size-scaling of phytoplankton metabolism follows the general allometric rule is necessary not only to verify if broad macroecological patterns are valid across all domains of life (DeLong et al., 2012) but also to identify the ultimate mechanisms that control the spatial and temporal variability of phytoplankton size structure in the sea (Chisholm, 1992; Kiørboe, 1993). Since cell size is a key functional trait in phytoplankton, understanding its relationship with growth and metabolism is crucial to define the ecological strategies of different functional groups and how environmental forcing controls the assembly of communities in the ocean (Litchman et al., 2007).

We have studied the growth, biochemical composition, and carbon and nitrogen metabolism of 22 phytoplankton species grown in batch cultures. All cultures had the same conditions and all measurements were performed using the same protocol, thus avoiding methodological differences that may influence the results. Recently we have shown that phytoplankton metabolism does not follow Kleiber's power rule when cells are growing exponentially under optimal conditions (López-Sandoval et al., 2013; Marañón et al., 2013). Here we aim to determine if the same result holds for different growth phases, particularly when cells are experiencing nutrient deficiency, a situation that is often encountered in nature. In addition, we analyze the differences between taxonomic groups in terms of growth and carbon metabolism. Our results provide general patterns regarding the taxon- and cell size-dependence of metabolic rates, which has implications to understand the dynamics of phytoplankton community structure in the sea.

2. Methods

2.1. Phytoplankton cultures

A detailed description of culture conditions and the determination of cell abundance, size, and biomass have been given previously (López-Sandoval et al., 2013; Marañón et al., 2013). Briefly, the 22 phytoplankton species used for this study (Table 1) were grown in batch cultures at 18 ± 0.5 °C under an irradiance of 250 μmol photons m^{-2} s^{-1} provided by white light fluorescent tubes with a light:dark cycle of 12:12 h. Growth media were prepared with autoclaved, 0.2-μm filtered seawater collected from the Ría de Vigo (Spain). We used the f/4 medium for most species, K/2 medium for *Ostreococcus tauri* and *Micromonas pusilla*, and PCR-SC11/2 for *Prochlorococcus* sp. In all cases, nitrogen concentrations were modified so that the N/P molar ratio was ca. 6 and nitrogen limitation was ensured during the stationary growth phase. Cultures were acclimated to the temperature and irradiance conditions and to the growth medium for at least three transfers before the beginning of each experiment.

During the last growth cycle, daily samples were taken for determination of cell abundance, in vivo fluorescence, chlorophyll *a* concentration, biovolume, the photosystem II maximum photochemical efficiency

Table 1
Mean cell biovolume and biomass, photosystem II maximum quantum efficiency (F_v/F_m), carbon-specific total photosynthesis (P^C) and respiration (R^C), and the respiration to photosynthesis ratio (R:P) for each species during the exponential growth (Exp), and stationary (Sta) phases. P^C is also given for the intermediate (Int) phase. R:P is computed as $100 \times R^C / P^C$. Biomass data correspond to the mean value measured during all growth phases. NA, data not available.

Class	Species	Culture medium, NO^{3-}/NH_4^+	Biovolume (μm³)	Biomass (pgC cell^{-1})	F_v/F_m		P^C (h^{-1})			R^C (h^{-1})		R:P	
					Exp	Sta	Exp	Int	Sta	Exp	Sta	Exp	Sta
Bacillariophyceae	*Skeletonema costatum*	f/4, f/16[a]	242	22	NA	NA	0.14	0.13	0.16	0.004	0.007	2.5	4.3
Bacillariophyceae	*Thalassiosira rotula*	f/8, f/32[a]	2597	203	0.62	0.53	0.07	0.09	0.1	0.003	0.006	4	6
Bacillariophyceae	*Phaeodactylum tricornutum*	f/4, f/16[a]	93	5	0.63	0.33	0.2	0.15	0.03	0.003	0.002	1.3	7
Bacillariophyceae	*Thalassiosira weissflogii*	f/4, f/16[a]	1163	54	0.69	0.52	0.12	0.12	0.06	0.003	0.002	2.2	2.6
Bacillariophyceae	*Melosira nummuloides*	f/4, f/16[a]	2285	317	0.62	0.52	NA	NA	0.08	0.002	0.002	NA	2.6
Bacillariophyceae	*Coscinodiscus radiatus*	f/4, f/16[a]	81,955	3983	0.65	0.63	0.02	0.02	0.03	0.003	0.004	11.9	11
Bacillariophyceae	*Coscinodiscus wailesii*	f/4, f/16[a]	2,498,458	77,720	0.71	0.72	0.05	0.02	0.03	0.005	0.001	9.8	4.9
Bacillariophyceae	*Ditylum brightwellii*	f/4, f/16[a]	75,827	2551	0.6	0.6	0.05	0.05	0.04	0.003	0.004	9.5	9.9
Peridinea	*Protoceratium reticulatum*	L/2, L/8[b]	23,823	983	0.61	0.55	0.05	0.04	0.02	0.004	0.005	8.1	26.1
Peridinea	*Akashiwo sanguinea*	L/2, L/8[b]	47,349	2746	0.5	0.47	0.05	0.01	0.01	0.008	0.004	17.6	60.2
Peridinea	*Alexandrium minutum*	L/2, L/8[b]	5575	895	0.6	0.44	0.03	0.02	0.02	0.007	0.005	24.3	26.9
Peridinea	*Alexandrium tamarense*	L/2, L/8[b]	88,836	1435	0.57	0.47	0.04	0.03	0.02	0.01	0.008	26.6	49.6
Prymnesiophyceae	*Gephyrocapsa oceanica*	f/4, f/16[a]	82	12	0.66	0.62	0.17	0.08	0.03	0.005	0.005	3	17.2
Prymnesiophyceae	*Emiliania huxleyi*	f/4, f/16[a]	158	7.8	0.64	0.64	0.12	0.11	0.11	0.004	0.003	3.1	2.3
Prymnesiophyceae	*Calcidiscus leptoporus*	f/4, f/16[a]	51	4.2	0.67	0.53	NA	0.16	0.13	0.003	0.003	NA	2.6
Prymnesiophyceae	*Isochrysis galbana*	f/8, f/32[a]	64	4.6	0.68	0.55	0.1	0.05	0.03	0.007	0.004	6.6	12.2
Pavlovophyceae	*Pavlova lutheri*	f/4, f/16[a]	45	5.1	0.62	0.57	0.14	0.1	0.06	0.007	ND	5.4	NA
Eustigmatophyceae	*Nannochloropsis gaditana*	f/4, f/16[a]	8.6	2	0.57	0.56	0.07	0.04	0.03	0.005	0.002	7.4	8.1
Mamiellophyceae	*Micromonas pusilla*	K/2, K/8[c]	10.7	1.8	0.59	0.29	0.07	0.01	0.02	0.007	0.005	9.8	30.2
Mamiellophyceae	*Ostreococcus tauri*	K/2, K/8[c]	2.4	0.69	0.62	0.12	0.04	0.02	0.01	0.002	0.004	5.8	80.9
Cyanophyceae	*Synechococcus* sp.	f/4, f/16[a]	0.41	0.1	NA	NA	0.04	0.06	0.01	0.004	0.004	12.4	29.6
Cyanophyceae	*Prochlorococcus* sp.	PCR-S11, PCR-S11/4[d]	0.12	0.04	0.45	NA	0.02	0.01	0	0.002	0.003	11.9	67

[a] Guillard (1975).
[b] Guillard and Hargraves (1993).
[c] Keller and Guillard (1985).
[d] Roscoff Culture Collection's recipe.

(F_v/F_m), particulate organic carbon, particulate organic nitrogen, and dissolved inorganic nitrogen.

Chlorophyll *a* concentration was measured fluorometrically on a TD-700 Turner fluorometer after filtration of duplicate 5-mL samples onto GF/F filters, freezing of the filters at −20 °C and extraction with acetone. Biovolume measures where done with a Leica DLMB microscope using the NIS-Elements BR 3.0 image analysis software. We obtained critical cell dimensions in at least 100 cells by assigning different geometric shapes that were most similar to the real shape of each phytoplankton species (Sun and Liu, 2003). For particulate organic carbon and particulate organic nitrogen, duplicate 10-mL samples were filtered onto pre-combusted GF/F filters, which were stored at −20 °C. Prior to analysis, filters were kept in a desiccator at room temperature for 48 h. Samples were analyzed using a Carlo Erba Instruments EA 1108 elemental analyzer (CE Instruments Ltd, Wigan, UK) using acetanilide standard as a reference. Dissolved inorganic nitrogen concentration (NH_4^+ for *Prochlorococcus* sp. and NO_3^- for all other species) was measured following standard colorimetric methods. For F_v/F_m, triplicate samples were acclimated in the dark for 30 min and then variable fluorescence was determined using a Pulse Amplitude Modulated [Water PAM; Walz (Heinz Walz GmbH, Effeltrich, Germany)] fluorometer.

2.2. Metabolic activity

Following the daily cell counts and in vivo fluorescence measurements we determined three different sampling times within the growth cycle to evaluate metabolic rates at different physiological stages. The first sampling was during the exponential phase, defined as the initial point where cell densities were logarithmic increasing. We measured at an intermediate stage between exponential and stationary phases and the last sampling was performed during the stationary phase, when in general cell density remained relatively constant or started to decrease and dissolved inorganic nitrogen concentration was below 0.5 μmol L^{-1}.

2.2.1. Photosynthesis

Total photosynthetic production of organic carbon was measured with the ^{14}C-uptake after 2-h incubations in 20-mL glass vials. We used the filtrate recovery method, which allowed us to determine the production of both particulate organic carbon and dissolved organic carbon (López-Sandoval et al., 2013).

2.2.2. Respiration

Respiration was measured as oxygen consumption in the dark during the exponential growth and stationary phases. Six 50-mL borosilicate glass bottles were carefully filled using silicone tubing directly from the culture flask. Three bottles were fixed immediately for initial oxygen concentration and another three after incubation for 24 h. Dissolved oxygen was measured by automated precision Winkler titration using a potentiometric end point. Respiration rates were calculated as the difference between the initial and the final O_2 concentration. To calculate carbon-specific respiration, oxygen consumption rates were converted into carbon units by assuming that the molar O_2 consumption to CO_2 release ratio was 1.4 (Anderson and Sarmiento, 1994).

2.3. Statistical analysis

To obtain the slope and the intercept of the scaling relationship between metabolic rates and cell size, a reduced major axis analysis was performed. The 95% confidence intervals for the size-scaling parameters were calculated by bootstrapping over cases (2000 repetitions). The comparison of the slope values obtained with expected values (1 and 3/4) was done with a Student's t-test following Clarke's method (Clarke, 1980). The optimal model selection was determined by applying the Akaike information criterion (AIC) (Akaike, 1974). Due to non-normal distribution of the data, a non-parametric test (Kruskal–Wallis) was used to assess the presence of statistically significant differences among groups. The non-parametric Mann–Whitney test was used to compare the means between groups.

3. Results

3.1. Size-scaling of photosynthesis and respiration

Cell size, expressed either as volume or carbon per cell, was a very good predictor of cell-specific photosynthesis and respiration rates during all three growth phases, as it explained around 95% of the observed variability (Figs. 1 and 2; Table 2). The slopes in the size-scaling relationship of both metabolic rates were always significantly higher than 0.75 and, in most cases, were not different from 1 (Table 2), implying an isometric or near-isometric relationship between metabolic rate and cell size. When cell size was expressed as cell volume, the slope of the size-scaling relationship for both photosynthesis and respiration was approximately 0.9. However, when it was expressed as cell carbon, slope values were not significantly different from 1

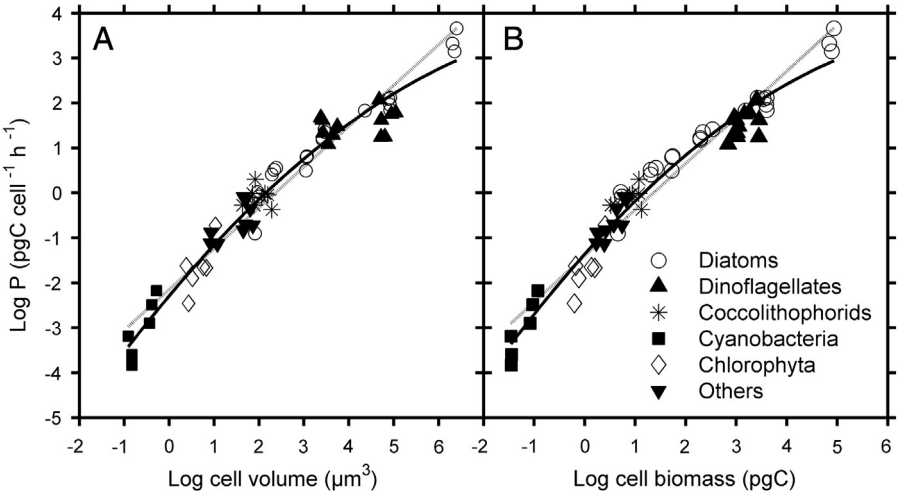

Fig. 1. Relationship between log cell-specific photosynthesis rate and log cell size measured as A) cell biovolume and B) cell biomass, with data from all growth phases combined. The light line is the reduced major axis (r.m.a) linear regression and the solid line is the quadratic fit. The linear models are A) y = 0.91 (0.03) x − 2.14 (0.09) and B) y = 1.03 (0.03) x − 1.40 (0.07). In both cases, $r^2 = 0.94$ and $n = 63$. The quadratic fits are: A) y = 1.19 (0.07) x − 0.06 (0.001) x^2 − 2.29 (0.09); B) 1.26 (0.006) x − 0.08 (0.01) x^2 − 1.37 (0.06). $r^2 = 0.96$ and $n = 63$ in both cases. Standard errors are given in parentheses.

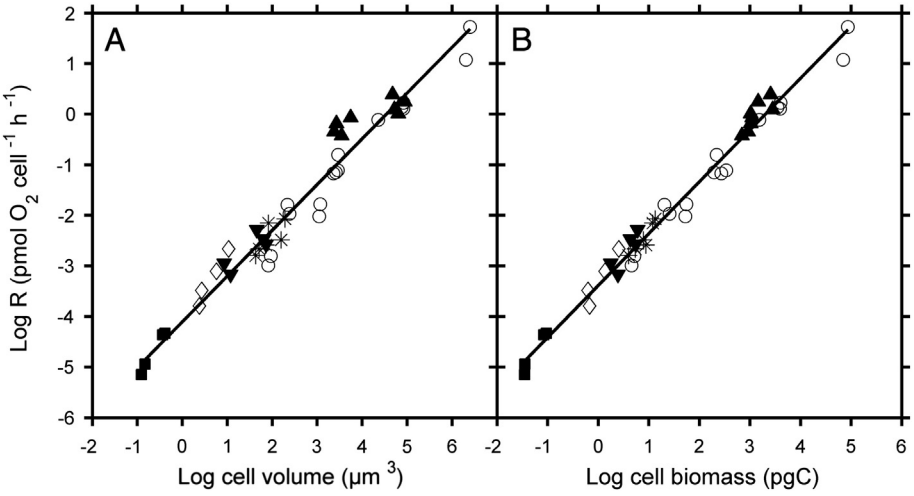

Fig. 2. Relationship between log cell-specific respiration rate and log cell size measured as A) cell biovolume and B) cell biomass, with data from both growth phases combined. The fitted line is the r.m.a linear regression. The linear models are: A) y = 0.9 (0.03) x − 4.1 (0.09), $r^2 = 0.96$, $n = 43$; B) y = 1.02 (0.02) x − 3.4 (0.05), $r^2 = 0.98$, $n = 43$. Symbols as in Fig. 1.

(Table 2). The significant departure of the size-scaling slopes from the value of 3/4, as well as the differences in slope values depending on whether volume or carbon was used as the measure of cell size, were consistently found in all growth phases (Table 2).

Although the linear model explained a large amount of the size-related variability in both metabolic rates, the log–log representation masked the existence of curvature in the size-scaling of photosynthesis. Using a quadratic function to fit the relationship between photosynthetic rate and cell size, the fit improved by explaining an additional 2% of the total variability (Fig. 1). More importantly, this quadratic fit resulted in lower AIC values (53 vs. 73 for biovolume and 46 vs. 68 for biomass) and in an even distribution of the residuals, whereas in the case of the linear model the residuals described a dome-shaped distribution (data not shown). The presence of curvature in the size-scaling of metabolic rates was more evident when carbon-specific photosynthesis (P^C) rates were plotted against cell size using a semilog representation (Fig. 3). If a single, scale-free power law was capturing adequately the size-dependence of metabolic rate, the relationship between biomass- (or volume-) specific metabolic rate and cell size should display the same slope throughout the entire cell size range. In contrast, we found that the slope of the P^C versus cell size relationship was positive in the small-to-medium cell size range and negative in the medium-to-large cell size range. This unimodal pattern, present in all growth phases, was particularly evident during the exponential growth phase (Fig. 3A). P^C rates ranged between approximately 0.01 and 0.2 h^{-1}, with the highest values (>0.1 h^{-1}) being measured in intermediate-size species (Fig. 3).

Respiration was markedly lower than photosynthesis, typically ranging between 0.001 and 0.01 h^{-1} (Fig. 4A, B), and did not show any size-related pattern. The respiration to photosynthesis ratio (R:P) took values below 15% in most species during the exponential phase (Fig. 4C), but increased during the stationary phase, particularly in the dinoflagellates, cyanobacteria, and chlorophytes, reaching values >25% (Table 1, Fig. 4D). For all species pooled together, the mean R:P ratio was 9 ± 7% during the exponential growth phase and 22 ± 23% during the stationary phase (Table 3).

3.2. The effect of growth phase and taxonomic affiliation

Taking all species into account, P^C rates during the exponential growth phase (0.08 ± 0.05 h^{-1}, mean ± standard deviation) were significantly higher than those during the stationary phase (0.05 ± 0.04 h^{-1}) (Kruskal–Wallis test, $X^2 = 6.12$, $p = 0.04$) (Fig. 3, Tables 1 and 3). The decrease in photosynthetic performance during the stationary phase was also evident, for most species, in F_v/F_m, which on average decreased by 17% (Table 1). By taxonomic group, the highest P^C rates corresponded to coccolithophorids, whose mean values ranged from 0.14 ± 0.04 h^{-1} during the exponential growth phase to 0.09 ±

Table 2
Parameters of the size-scaling relationships for photosynthesis and respiration rates during the exponential growth (Exp), intermediate (Int), and stationary (Sta) phases. Reduced major axis (r.m.a.) regression was used to determine the relationship between the logarithm of phytoplankton cell volume (μm^3) and biomass (pgC) and the logarithm of cell-specific photosynthesis (P, pgC $cell^{-1}$ h^{-1}) and respiration (R, pmol O_2 $cell^{-1}$ h^{-1}). Bootstrap 95% confidence intervals for the intercept and the slope are given in parentheses. *p* values refer to the comparison (Student's t-test following Clarke's method) of the size-scaling slope with the expected values of 0.75 and 1.0.

Metabolic rate	Cell size measure	*n*	r.m.a. slope	95% CI	Intercept	95% CI	r^2	Slope = 0.75	Slope = 1
								p	*p*
P (Exp)	μm^3	20	0.87	(0.8, 0.9)	−1.86	(−2.1, −1.5)	0.96	0.004	<0.01
P (Int)	μm^3	21	0.88	(0.8, 1.0)	−2.10	(−2.3, −1.7)	0.95	<0.001	0.02
P (Sta)	μm^3	22	0.96	(0.8, 1.0)	−2.44	(−2.7, −2.0)	0.93	<0.001	0.51
P (all)	μm^3	63	0.91	(0.8, 0.9)	−2.14	(−2.3, −1.9)	0.94	<0.001	<0.01
P (Exp)	pgC $cell^{-1}$	20	0.99	(0.9, 1.1)	−1.18	(−1.4, −1.0)	0.97	<0.001	0.78
P (Int)	pgC $cell^{-1}$	21	1.00	(0.9, 1.1)	−1.35	(−1.6, −1.0)	0.94	<0.001	1.00
P (Sta)	pgC $cell^{-1}$	22	1.08	(0.9, 1.2)	−1.64	(−1.9, −1.3)	0.94	<0.001	0.16
P (all)	pgC $cell^{-1}$	63	1.03	(0.9, 1.1)	−1.40	(−1.5, −1.2)	0.94	<0.001	0.37
R (Exp)	μm^3	22	0.92	(0.8, 1.0)	−4.10	(−4.3, −3.8)	0.96	<0.001	0.04
R (Sta)	μm^3	21	0.89	(0.8, 1.0)	−4.10	(−4.3, −3.8)	0.96	<0.001	0.02
R (all)	μm^3	43	0.90	(0.8, 0.9)	−4.10	(−4.2, −3.9)	0.96	<0.001	<0.01
R (Exp)	pgC $cell^{-1}$	22	1.04	(1.0, 1.1)	−3.39	(−3.5, −3.2)	0.99	<0.001	0.12
R (Sta)	pgC $cell^{-1}$	21	1.01	(0.9, 1.1)	−3.38	(−3.5, −3.2)	0.98	<0.001	0.86
R (all)	pgC $cell^{-1}$	43	1.02	(1.0, 1.1)	−3.38	(−3.5, −3.3)	0.98	<0.001	0.26

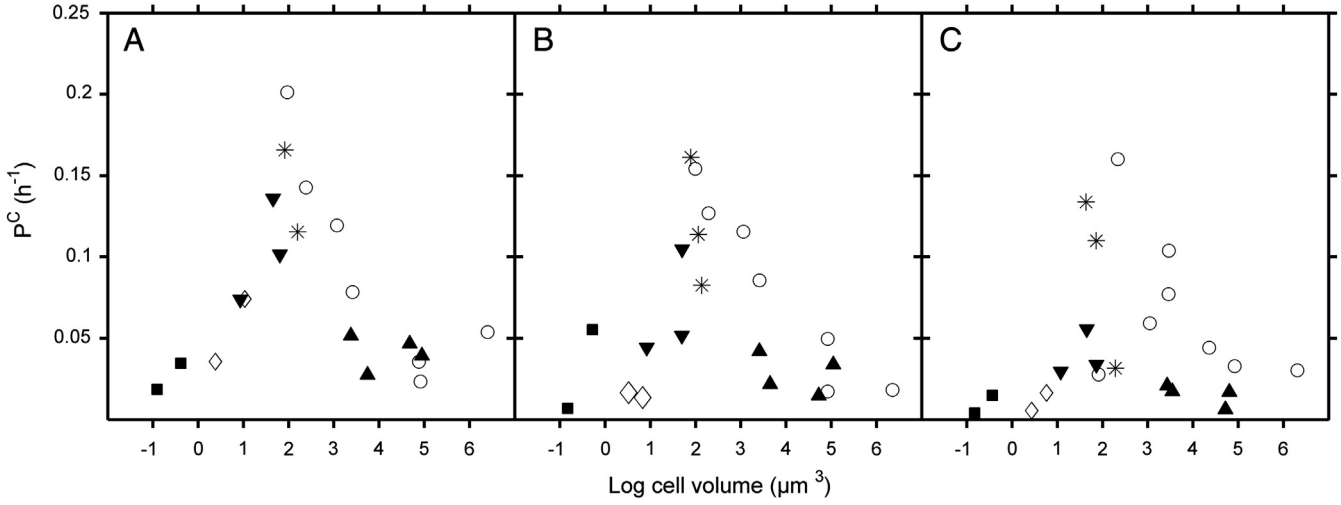

Fig. 3. Size-dependence of carbon-specific photosynthesis (P^C) measured during the A) exponential growth, B) intermediate, and C) stationary phases. Symbols as in Fig. 1.

0.05 h^{-1} during the stationary phase (Tables 1 and 3). Diatoms showed somewhat lower values, ranging between 0.07 ± 0.05 h^{-1} during the stationary phase and 0.09 ± 0.06 h^{-1} during exponential growth. Dinoflagellates and cyanobacteria presented the lowest P^C rates, with values between 0.01 and 0.04 h^{-1}. However, these between-group differences were significant only during the stationary phase, when diatoms had significantly higher P^C values (0.07 ± 0.05 h^{-1}) than dinoflagellates, cyanobacteria and chlorophytes (Mann Whitney U-test, $p = 0.04$ in all cases) (Tables 1 and 3).

Contrary to photosynthesis, carbon-specific respiration (R^C) rates were relatively constant between growth phases (Fig. 4A, B; Table 1). Overall, taking all species into account, no significant differences were observed between growth phases (Kruskal–Wallis test, $X^2 = 0.40$, $p = 0.53$). Group-specific, mean R^C values ranged between 0.003 and 0.007 h^{-1} during the exponential phase and between 0.003 and 0.006 h^{-1} during the stationary phase (Table 3). Differences between groups were significant during the exponential growth phase (Kruskal–Wallis test, $X^2 = 13.9$, $p = 0.02$), when dinoflagellates had significantly higher respiration rates (0.007 ± 0.003 h^{-1}) than coccolithophorids (0.004 ± 0.001 h^{-1}) and diatoms (0.003 ± 0.001 h^{-1}) (Mann Whitney U-test, $p = 0.03$ in both cases) (Table 3). During the stationary phase, dinoflagellates still showed the highest respiration rates of all groups, although the differences were not significant (Kruskal–Wallis test, $X^2 = 5$, $p = 0.4$).

The group-specific respiration to photosynthesis ratio (R:P) increased from the exponential growth phase to the stationary phase, except in the case of diatoms, whose R:P values remained relatively unchanged (around 6%) (Table 3). The differences in R:P observed between groups during the stationary phase were significant (Kruskal–Wallis test, $X^2 = 15.22$, $p = 0.01$). During this phase, diatoms had lower R:P (6 ± 3%) than dinoflagellates (41 ± 17%), cyanobacteria (48 ± 26%) and chlorophytes (55 ± 36%) (Mann–Whitney U-test,

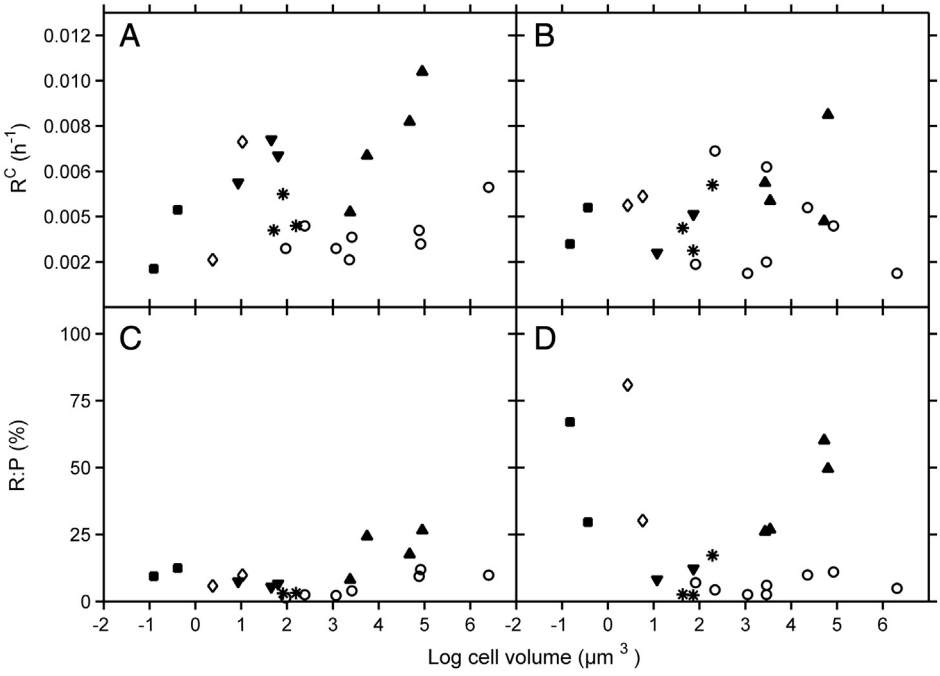

Fig. 4. Size-dependence of (A, B) carbon-specific respiration (R^C) and (C, D) the respiration to photosynthesis ratio (R:P) during the exponential growth phase (A, C) and the stationary phase (C, D). Symbols as in Fig. 1.

Table 3
Carbon-specific photosynthesis (P^C) and respiration (R^C) rates and the respiration to photosynthesis ratio (R:P) for each taxonomic group during the different growth phases. *n* is the number of data (species) available in each case. SD is the standard deviation.

	Taxonomic group	Exponential			Intermediate			Stationary		
		n	Mean	SD	*n*	Mean	SD	*n*	Mean	SD
P^C (h^{-1})	Diatoms	7	0.09	0.06	7	0.08	0.05	8	0.07	0.05
	Dinoflagellates	4	0.04	0.01	4	0.03	0.01	4	0.02	0.01
	Coccolithophorids	2	0.14	0.04	3	0.12	0.04	3	0.09	0.05
	Cyanobacteria	2	0.03	0.01	2	0.03	0.03	2	0.01	0.01
	Chlorophytes	2	0.05	0.03	2	0.02	0.00	2	0.01	0.01
	Others	3	0.10	0.03	3	0.07	0.03	3	0.04	0.01
	All species	20	0.08	0.05	21	0.06	0.05	22	0.05	0.04
R^C (h^{-1})	Diatoms	8	0.003	0.001				8	0.003	0.002
	Dinoflagellates	4	0.007	0.003				4	0.006	0.002
	Coccolithophorids	3	0.004	0.001				3	0.004	0.001
	Cyanobacteria	2	0.003	0.002				2	0.004	0.001
	Chlorophytes	2	0.005	0.004				2	0.005	0.000
	Others	3	0.007	0.001				2	0.003	0.001
	All species	22	0.005	0.002				21	0.004	0.002
R:P	Diatoms	7	5.9	4.4				8	6.0	3.1
	Dinoflagellates	4	19.2	8.3				4	40.7	17.0
	Coccolithophorids	2	3.1	0.1				3	7.4	8.5
	Cyanobacteria	2	10.9	2.2				2	48.3	26.5
	Chlorophytes	2	7.8	2.9				2	55.5	35.9
	Others	3	6.5	1.0				2	10.2	2.9
	All species	20	9.2	7.0				21	22.0	23.5

$p < 0.05$ in all cases), while dinoflagellates exhibited significantly higher R:P than coccolithophorids (7 ± 8%) (Mann–Whitney U-test, $p < 0.001$) (Table 3).

We calculated, for both photosynthesis and respiration, the ratio between the rates measured during the stationary phase (P^C_{sta} and R^C_{sta}) and the corresponding rates measured during the exponential growth phase (P^C_{exp} and R^C_{exp}) (Fig. 5). For most species, especially those in the smaller half of the size range considered, P^C_{sta}:P^C_{exp} took values well below 0.5 (Fig. 5A), indicating that for these species entering the stationary phase led to a marked decrease in photosynthetic carbon fixation rates, compared to those sustained during exponential growth. In contrast, in several medium- and large-sized species, including the coccolithophore *Emiliania huxleyi* and four diatoms, P^C_{sta}:P^C_{exp} took values near or even above 1, indicating that carbon fixation during the stationary phase proceeded at rates similar to or even higher than those attained during exponential growth. The values of R^C_{sta}:R^C_{exp} were, in general, higher than 0.5 and in several species they reached values above 1.5, indicating a marked increase in biomass-specific respiration rates upon entering the stationary phase (Fig. 5B).

In contrast to the pattern observed in P^C_{sta}:P^C_{exp}, there was no obvious relationship between cell size and R^C_{sta}:R^C_{exp}. Pooling data by taxonomic affiliation showed that in most groups carbon fixation rates were markedly depressed (by 60–80%) during the stationary phase (Fig. 6). Diatoms and coccolithophorids were an exception to this pattern, as they showed an average reduction of P^C of only 28% and 35% respectively. In the case of group-specific changes in respiration, in most cases R^C was maintained or increased moderately during the stationary phase (Fig. 6).

4. Discussion

By conducting direct measurements on phytoplankton cultures growing under identical conditions and using standardized protocols we have avoided the uncertainties of meta-analysis studies, which include data, often obtained with different procedures, from cultures experiencing disparate growth conditions. As a result, we have obtained size-scaling relationships for both photosynthesis and respiration which show remarkably high regression coefficients and therefore represent robust macroecological patterns. In addition, we have determined metabolic rates during different phases along the growth cycle, which allowed us to investigate to which extent the size-scaling of phytoplankton metabolism is dependent on the physiological state of the populations, as well as to identify differences between taxonomic groups in the growth phase-dependent dynamics of photosynthesis and respiration.

4.1. Isometric size-scaling of metabolic rate

Our results demonstrate that the size-scaling of phytoplankton metabolism does not follow the 3/4-power rule, but instead is isometric or nearly isometric. The relationship between cell size and both photosynthesis and respiration was largely independent of the population's physiological state, because similar slope values were obtained in the different growth phases studied. These observations are in contrast to previous studies, which reported that the size-scaling exponent for phytoplankton metabolic rates was equal or close to 3/4 (Blasco et al., 1982; López-Urrutia et al., 2006; Taguchi, 1976). One possible reason for this discrepancy is that cultures are often grown to very high biomass concentrations, whereas in our study we used growth media with a reduced amount of nitrogen and therefore the cell densities attained were smaller. The use of very dense cultures and low irradiances may lead to algal light limitation which, as a result of the package effect, is known to affect more severely larger cells and thus result in lower size-scaling exponents (Finkel et al., 2004). Another key factor is that previous laboratory-based studies did not include species below 100 μm^3 in cell volume. Our own data indicate that when only species larger than 100 μm^3 are considered, the scaling of photosynthesis is indeed allometric ($b = 0.74$; 95% CI = 0.59–0.78). Hence, the overall isometric size-scaling pattern only arises when small (e.g. <100 μm^3 in cell volume) species are considered together with intermediate- and large-sized species.

The value of the size-scaling exponent for a given metabolic rate depends critically on whether biomass (e.g., carbon) or biovolume is used as a metric for phytoplankton cell size. For instance, it has been reported that the value of the size-scaling exponent for phytoplankton photosynthesis was 1.05 when cell biomass was used as a metric for cell size and 0.74 when cell size was expressed as cell volume (López-Urrutia et al., 2006). These results, however, rested on the assumption that carbon density in phytoplankton decreases very fast with increasing cell size, as implied in the use of Strathmann's equation, where cell carbon (C) is a function of cell volume (V) such that $C \propto V^{0.71}$ (Strathmann, 1967). Several, more recent studies have shown that in fact the decrease

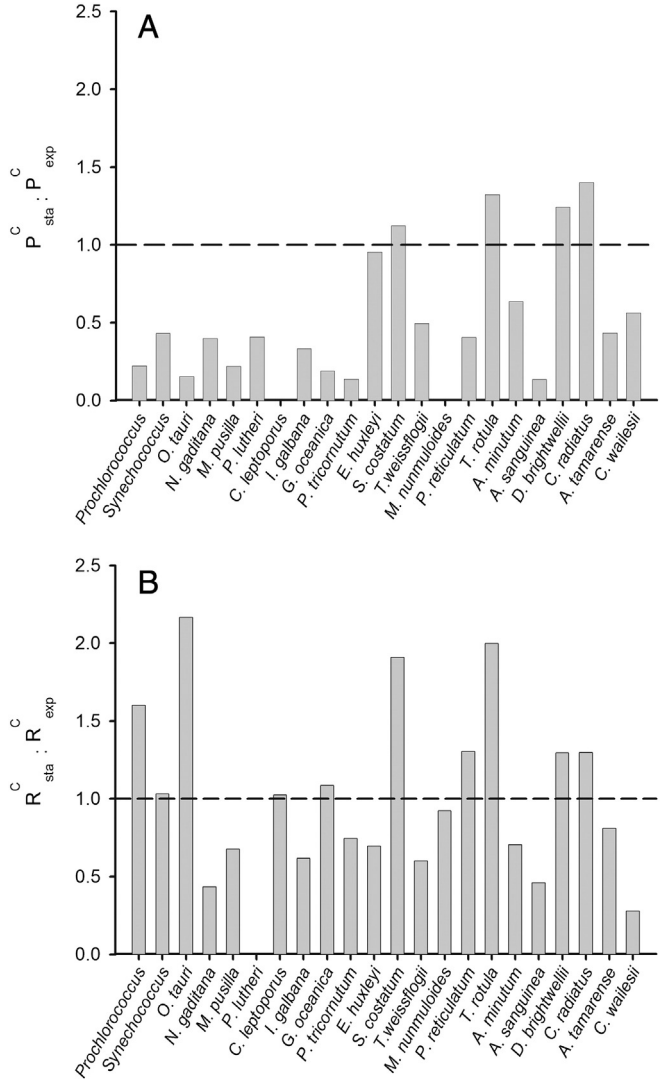

Fig. 5. A) Ratio between carbon-specific photosynthesis rates measured during the stationary phase (P^C_{sta}) and during the exponential growth phase (P^C_{sta}). B) As in A) but for carbon-specific respiration (R^C) rate. Species are arranged in an increasing order of cell volume.

in carbon density with increasing cell size is much less dramatic, as the scaling exponent in the power relationship relating C to V takes values around 0.9 (Menden-Deuer and Lessard, 2000). In our own cultures, $C \propto V^{0.88}$ (Marañón et al., 2013) and the size-scaling exponent of photosynthesis was around 1 and 0.9 when C and V, respectively, were used as a metric for cell size. In conclusion, size-related changes in cell carbon density do not alter the fact that phytoplankton metabolic rates do not scale allometrically as predicted by the 3/4-power rule.

An isometric size-scaling pattern implies that both small and large phytoplankton species are capable of sustaining similar mass- or volume-specific metabolic rates, thus negating the expected monotonic slowdown of metabolism as cell size increases. Scaling arguments suggest that the best evolutionary strategy for phytoplankton is to minimize cell size in order to maximize the surface to volume ratio, avoid nutrient diffusion limitation, and reduce cell losses through sinking (Raven, 1998). Increasing cell size leads to more intense self-shading (Finkel et al., 2004), a thicker boundary layer, and an increase in the average transport distance within the cell (Kiørboe, 1993), making diffusion inadequate to maintain a constant solute concentration throughout the cytosol (Beardall et al., 2009). However, large cells possess several traits which may help them to counterbalance the physiological constraints imposed by their size. These include changes in cell shape (e.g., the ellipsoidal shape in pennate diatoms), enhanced nutrient storage capacity (Litchman et al., 2007), and a reduction in volume-specific nutrient requirements (Thingstad et al., 2005). Additional work conducted with the same cultures described here has shown that the maximum nitrogen uptake rate (V_{maxN}) scales isometrically with cell volume, whereas the minimum nitrogen quota scales allometrically (Marañón et al., 2013). As a result, larger species have an increased ability to acquire nutrients, relative to their requirements, when nutrients are available in large amounts. The high biomass-specific V_{maxN} and nutrient storage ability of large cells make them particularly well-adapted to exploit transient situations of enhanced nutrient supply.

4.2. Curvature in metabolic size-scaling

Size-scaling studies often rely on the analysis of the log–log relationship between individual metabolic rates and body size. Provided that the range of organism size is sufficiently wide, these relationships typically conform to a linear regression model with a high regression coefficient, which makes it easy to overlook the existence of non-linearities. This is

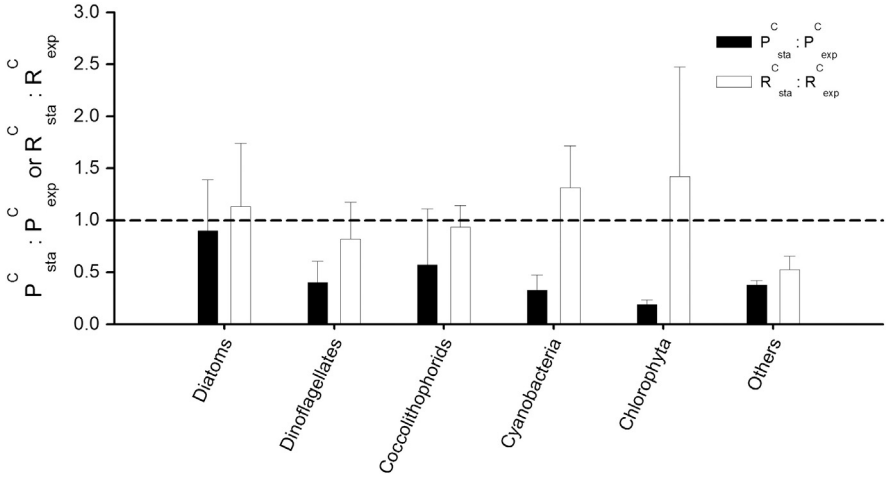

Fig. 6. Ratio between the rates of carbon-specific photosynthesis (P^C) or respiration (R^C) measured during the stationary phase and those measured during the exponential growth phase for each taxonomic group. Vertical bars indicate the standard deviation.

illustrated in our data by the fact that, in spite of the high regression coefficient in the relationships between the logarithms of cell-specific photosynthesis rates and cell size, the size-dependence of carbon-specific photosynthesis (P^C) was strongly non-linear, with intermediate-size cells sustaining the fastest metabolism. The presence of curvature in the size-scaling of metabolic rates indicates that different biophysical and physiological constraints are operating along the size range considered (Kolokotrones et al., 2010). In our cultures, measurements of carbon and nitrogen stoichiometry together with nitrogen maximum uptake rates suggest that the unimodality in P^C is caused by changes in nutrient requirement, uptake and use along the size spectrum (Marañón et al., 2013).

The small species in our study had lower carbon to nitrogen ratios, indicating that they were comparatively more nitrogen-rich, and therefore had higher nitrogen requirements, than their larger counterparts (Marañón et al., 2013). In addition, the cellular space occupied by non-scalable components (such as membranes and nucleic acids) increases with decreasing cell size, which means that picophytoplankton cells have a more limited amount of space to accommodate the catalysts involved in the synthesis of new biomass (Beardall et al., 2009; Raven, 1998). Thus, in the small to medium size range, biomass-specific photosynthesis would increase with cell size because nitrogen requirements decrease and also because more space becomes available for the enzymes involved in biomass synthesis. In the medium-to-large size range, metabolism would slow down, in spite of the cells' large nutrient uptake ability, as a result of the increasingly large intracellular distances for the transport of resources from the cell membrane (Banavar et al., 2002). These contrasting limiting factors in small and large species would thus lead to the observed unimodal pattern in biomass-specific carbon fixation rates, which contributes to explain the fact that phytoplankton blooms in the ocean tend to be dominated by intermediate-size species rather than very small or very large ones.

4.3. Size- and taxon-related variability in respiration

The size-scaling of phytoplankton respiration has been analyzed before in species within a cell volume range of approximately 10 to 10^4 μm^3. Most of these studies have shown that respiration scales with cell volume with an exponent higher than 3/4, indicating a smaller degree of size-dependence than predicted by Kleiber's rule (Banse, 1976; Lewis, 1989; Tang and Peters, 1995). Our results confirm this pattern over a much wider size range (0.1 to 10^6 μm^3), and thus provide additional evidence to negate the view that size-related differences in respiratory losses may contribute to explain the patterns of phytoplankton size structure in the sea (Laws, 1975). Contrary to photosynthesis, respiration did not show any sign of curvature in its size-scaling. Respiration in phytoplankton thus appears as a more conservative process than photosynthesis, showing a smaller degree of variability both across the cell size spectrum and between growth phases.

Dinoflagellates, which tend to suffer relatively high respiratory losses (Geider, 1992; Geider and Osborne, 1989), exhibited the highest mean respiration to photosynthesis ratio (19%) of all groups during exponential growth. The enhanced respiration rates in dinoflagellates could be related, in principle, to the energetic costs of motility. However, energetic budget analyses suggest that the costs of motility in protists represent only a small fraction of total metabolic expenditure (Crawford, 1992; Raven and Beardall, 1981). Alternatively, the cellular composition of dinoflagellates could explain their higher respiration rates. Compared to other algae, dinoflagellates contain a very large amount of genetic material, which may lead to higher energetic costs involved in DNA and RNA turnover (Rizzo, 2003). An additional factor which can contribute to higher respiration is that the flagellar membrane in these organisms is not covered by the cell wall, which imposes a constant expenditure of energy for volume and osmotic regulation (Raven and Beardall, 1981).

During the stationary phase, cyanobacteria and chlorophytes, together with dinoflagellates, showed the highest respiratory losses (>40% of photosynthetically fixed carbon). The cyanobacteria and chlorophytes studied here were all very small cells (less than approximately 10 μm^3 in cell volume) and had a comparatively small nutrient storage capacity. Hence, these species may have suffered more from nutrient exhaustion during the stationary phase and turned to macromolecule turnover as a source of energy, thus incurring in higher respiratory losses.

4.4. Differences in carbon metabolism between growth phases

We found that, in general, P^C tends to decrease markedly during the stationary phase, indicating a reduction in photosynthetic carbon fixation, presumably induced by nutrient exhaustion in the external medium. Although in most of the species we observed a decrease in photosynthetic performance during the stationary phase, our results showed that the efficiency of photosystem II (indicated by F_v/F_m) has a species-specific response to nutrient limitation (as shown by Kruskopf and Flynn (2006)) which might be related to different physiological acclimation capacities (Claquin et al., 2010). The F_v/F_m ratio has been extensively use as an indicator of nutrient stress, however, our data supports the view that this ratio does not always give a robust index of nutrient status (Parkhill et al., 2001). In contrast to photosynthesis, R^C remained relatively unchanged, and as a result its relative importance for the overall cellular carbon budget increased during the stationary phase. Overall, our measurements suggest that the range of variation in biomass-specific respiration is smaller than that in biomass-specific photosynthesis and that the coupling between carbon fixation and respiration is rather loose (Geider, 1992).

Diatoms represented an exception to the general pattern of decreased P^C during the stationary phase. In this phase, many diatom species were able to sustain high rates of biomass-specific carbon fixation, despite nitrogen exhaustion in the external medium. As a result, they tended to show increased carbon to nitrogen ratios in their biochemical composition (Marañón et al., 2013), which probably resulted from intracellular carbohydrate accumulation. The fact that diatoms keep fixing carbon after nutrients are no longer available, together with their ability to take up nutrients at very fast rates when they are in high supply (Marañón et al., 2013), allow them to uncouple carbon and nutrient uptake, which is likely to represent a competitive advantage when nutrient delivery is discontinuous (Cermeño et al., 2011; Falkowski and Oliver, 2007).

4.5. Concluding remarks

We have shown unequivocally that, irrespective of the growth conditions, the size-scaling of phytoplankton photosynthesis and respiration cannot be predicted by Kleiber's rule. A single, overall isometric model gives a good approximation to the size-scaling of phytoplankton metabolism, because both large and small species sustain similar rates. However, the observed curvature in metabolic scaling means that intermediate-size species can attain faster biomass-specific metabolic rates, and are thus more likely to form blooms. In addition, we have found significant taxon-related differences in metabolic rates. Relative to other groups, dinoflagellates have higher respiratory losses, whereas diatoms are capable of sustaining relatively high biomass-specific carbon fixation rates during conditions of nutrient limitation.

Author contributions

EM and PC designed the study; DCL-S and TR-R conducted the experiments and obtained data; DCL-S, TR-R and EM analyzed the data; DCL-S and EM wrote the article; all authors discussed the results and commented on the manuscript.

Acknowledgments

We thank M. P. Lorenzo and A. Fernández for assistance in the laboratory and J. M. Blanco, R. Palomino, and J. Rodríguez for the flow cytometry data. D.C.L.S. was supported by a postgraduate fellowship from the Mexican Council of Science and Technology (CONACyT) and the Xunta de Galicia (Spain). This research was funded by the Spanish Ministerio de Ciencia e Innovación through the Ciencias y Tecnologías Marinas research project 'Macroecological patterns in marine phytoplankton' (Grant CTM2008-03699/MAR to E.M.). **[SS]**

References

Akaike, H., 1974. A new look at the statistical model identification. IEEE Trans. Autom. Control 19 (6), 716–723.
Anderson, L.A., Sarmiento, J.L., 1994. Redfield ratios of remineralization determined by nutrient data analysis. Glob. Biogeochem. Cycles 8 (1), 65–80.
Armstrong, R.A., 1994. Grazing limitation and nutrient limitation in marine ecosystems: steady state of an ecosystem model with multiple food chains. Limnol. Oceanogr. 39, 597–608.
Banavar, J.R., Damuth, J., Maritan, A., Rinaldo, A., 2002. Supply-demand balance and metabolic scaling. Proc. Natl. Acad. Sci. U. S. A. 99 (16), 10506–10509.
Banse, K., 1976. Rates of growth, respiration and photosynthesis of unicellular algae as related to cell size: a review. J. Phycol. 12, 135–140.
Beardall, J., Allen, D., Bragg, J., Finkel, Z.V., Flynn, K.J., Quigg, A., Rees, T.A.V., Richardson, A., Raven, J.A., 2009. Allometry and stoichiometry of unicellular, colonial and multicellular phytoplankton. New Phytol. 181 (2), 295–309.
Blasco, D., Packard, T.T., Garfield, P.C., 1982. Size dependence of growth rate, respiratory electron transport system activity, and chemical composition in marine diatoms in the laboratory. J. Phycol. 18 (1), 58–63.
Brown, J.H., Gillooly, J.F., Allen, A.P., Savage, V.M., West, G.B., 2004. Toward a metabolic theory of ecology. Ecology 85 (7), 1771–1789.
Cermeño, P., Lee, J.-B., Wyman, K., Schofield, O.M., Falkowski, P.G., 2011. Competitive dynamics in two species of phytoplankton under non-equilibrium conditions. Mar. Ecol. Prog. Ser. 429, 19–28.
Chisholm, S.W., 1992. Phytoplankton size. In: Falkowski, P.G. (Ed.), Primary Productivity and Biogeochemical Cycles in the Sea. Plenum Press, New York and London, pp. 213–237.
Claquin, P., Ní Longphuirt, S., Fouillaron, P., Huonnic, P., Ragueneau, O., Klein, C., Leynaert, A., 2010. Effects of simulated benthic fluxes on phytoplankton dynamic and photosynthetic parameters in a mesocosm experiment (Bay of Brest, France). Estuar. Coast. Shelf Sci. 86 (1), 93–101.
Clarke, M.R.B., 1980. The reduced major axis of a bivariate sample. Biometrika 67, 441–446.
Crawford, D.W., 1992. Metabolic cost of motility in planktonic protists: theoretical considerations on size scaling and swimming speed. Microb. Ecol. 24 (1), 1–10.
DeLong, J.P., Okie, J.G., Moses, M.E., Sibly, R.M., Brown, J.H., 2012. Shifts in metabolic scaling, production, and efficiency across major evolutionary transitions of life. Proc. Natl. Acad. Sci. U. S. A. 107 (29), 12941–12945.
Falkowski, P.G., Oliver, M.J., 2007. Mix and match: how climate selects phytoplankton. Nat. Rev. Microbiol. 5 (10), 813–819.
Finkel, Z.V., Irwin, A.J., Schofield, O., 2004. Resource limitation alters the 3/4 size scaling of metabolic rates in phytoplankton. Mar. Ecol. Prog. Ser. 273, 269–279.
Finkel, Z.V., Beardall, J., Flynn, K.J., Quigg, A., Rees, T.A.V., Raven, J.A., 2010. Phytoplankton in a changing world: cell size and elemental stoichiometry. J. Plankton Res. 32 (1), 119–137.
Geider, R.J., 1992. Respiration: taxation without representation? In: Falkowski, P.G., Woodhead, A.D. (Eds.), Primary Productivity and Biogeochemical Cycles in the Sea. Plenum Press, New York and London, pp. 333–360.
Geider, R.J., Osborne, B.A., 1989. Respiration and microalgal growth: a review of the quantitative relationship between dark respiration and growth. New Phytol. 112, 327.
Guillard, R.R.L., 1975. Culture of phytoplankton for feedingmarine invertebrates. In: Smith, W.L., Chanley, M.H. (Eds.), Culture of marine invertebrate animals. Plenum, NewYork, NY.
Guillard, R., Hargraves, P., 1993. Stichochrysis immobilis is adiatom, not a chrysophyte. Phycologia 32, 234–236.
Huete-Ortega, M., Cermeño, P., Calvo-Díaz, A., Marañón, E., 2012. Isometric size-scaling of metabolic rate and the size abundance distribution of phytoplankton. Proc. R. Soc. B Biol. Sci. 279 (1734), 1824–1830.
Irwin, A.J., Finkel, Z.V., Schofield, O.M., Falkowski, P.G., 2006. Scaling-up from nutrient physiology to the size-structure of phytoplankton communities. J. Plankton Res. 28 (5), 459–471.
Keller, M., Guillard, R., 1985. Factors significant to marinedinoflagellate culture. In: Anderson, D.M., White, A.W., Baden, D.G. (Eds.), Toxic dinoflagellates. Elsevier, New York, NY, pp. 113–116.
Kiørboe, T., 1993. Turbulence, phytoplankton cell size, and the structure of pelagic food webs. Adv. Mar. Biol. 29 (29), 1–72.
Kleiber, M., 1932. Body size and metabolism. Hilgardia 6, 315–353.
Kolokotrones, T., Savage, V., Deeds, E.J., Fontana, W., 2010. Curvature in metabolic scaling. Nature 464 (7289), 753–756.
Kruskopf, M., Flynn, K.J., 2006. Chlorophyll content and fluorescence responses cannot be used to gauge reliably phytoplankton biomass, nutrient status or growth rate. New Phytol. 169 (3), 525–536.
Laws, E.A., 1975. The importance of respiration losses in controlling the size distribution of marine phytoplankton. Ecology 56, 419–426.
Lewis, W.M., 1989. Further evidence for anomalous size scaling of respiration in phytoplankton. J. Phycol. 25 (2), 395–397.
Litchman, E., Klausmeier, C.A., Schofield, O.M., Falkowski, P.G., 2007. The role of functional traits and trade-offs in structuring phytoplankton communities: scaling from cellular to ecosystem level. Ecol. Lett. 10 (12), 1170–1181.
López-Sandoval, D.C., Rodríguez-Ramos, T., Cermeño, P., Marañón, E., 2013. Cell size- and taxon-dependence of organic carbon exudation in marine phytoplankton. Mar. Ecol. Prog. Ser. 477, 53–60.
López-Urrutia, A., San Martin, E., Harris, R.P., Irigoien, X., 2006. Scaling the metabolic balance of the oceans. Proc. Natl. Acad. Sci. U. S. A. 103 (23), 8739–8744.
Marañón, E., 2008. Inter-specific scaling of phytoplankton production and cell size in the field. J. Plankton Res. 30, 157–163.
Marañón, E., Cermeno, P., Rodriguez, J., Zubkov, M.V., Harris, R.P., 2007. Scaling of phytoplankton photosynthesis and cell size in the ocean. Limnol. Oceanogr. 52 (5), 2190–2198.
Marañón, E., Cermeño, P., López-Sandoval, D.C., Rodríguez-Ramos, T., Sobrino, C., Huete-Ortega, M., Blanco, J.M., Rodríguez, J., 2013. Unimodal size scaling of phytoplankton growth and the size dependence of nutrient uptake and use. Ecol. Lett. 16, 371–379.
Menden-Deuer, S., Lessard, E.J., 2000. Carbon to volume relationships for dinoflagellates, diatoms, and other protist plankton. Limnol. Oceanogr. 45, 569–579.
Parkhill, J.P., Maillet, G., Cullen, J.J., 2001. Fluorescence-based maximal quantum yield for PSII as a diagnostic of nutrient stress. J. Phycol. 37 (4), 517–529.
Raven, J.A., 1998. The twelfth Tansley Lecture. Small is beautiful: the picophytoplankton. Funct. Ecol. 12, 503–513.
Raven, J.A., Beardall, J., 1981. Respiration and photorespiration. In: Platt, T. (Ed.), Physiological Bases of Phytoplankton Ecology. Canadian Bulletin of Fisheries and Aquatic Sciences, Ottawa, pp. 55–82.
Rizzo, P.J., 2003. Those amazing dinoflagellate chromosomes. Cell Res. 13 (4), 215–217.
Savage, V.M., Gillooly, J.F., Woodruff, W.H., West, G.B., Allen, A.P., Enquist, B.J., Brown, J.H., 2004. The predominance of quarter-power scaling in biology. Funct. Ecol. 18 (2), 257–282.
Strathmann, R.R., 1967. Estimating the organic carbon content of phytoplankton from cell volume or plasma volume. Limnol. Oceanogr. 12, 411–418.
Sun, J., Liu, D., 2003. Geometric models for calculating cell biovolume and surface area for phytoplankton. J. Plankton Res. 25 (11), 1331–1346.
Taguchi, S., 1976. Relationship between photosynthesis and cell-size of marine diatoms. J. Phycol. 12 (2), 185–189.
Tang, E.P.Y., Peters, R.H., 1995. The allometry of algal respiration. J. Plankton Res. 17, 303–315.
Thingstad, T.F., Ovreas, L., Egge, J.K., Lovdal, T., Heldal, M., 2005. Use of non-limiting substrates to increase size; a generic strategy to simultaneously optimize uptake and minimize predation in pelagic osmotrophs? Ecol. Lett. 8 (7), 675–682.
Ward, B.A., Dutkiewicz, S., Jahn, O., Follows, M.J., 2012. A size-structured food-web model for the global ocean. Limnol. Oceanogr. 57 (6), 1877–1891.